Determination of InP HEMT Noise Parameters and S-Parameters to 60 GHz

Richard T. Webster, *Member, IEEE,* Andrew J. Slobodnik, Jr., *Member, IEEE,* and George A. Roberts

***Abstract*—A millimeterwave experimental technique is described for directly determining the noise parameters and scattering parameters of V-band InP HEMT's. The parameters are suitable for the design of monolithic millimeterwave integrated circuits since they represent the InP HEMT as it would appear in the monolithic environment. The method relies on careful characterization of the measurement system and the InP HEMT packages or test fixtures. Results are provided for an InP HEMT with 1.37 dB minimum noise figure and a maximum stable gain of 12.74 dB at 57 GHz. In addition, it is shown that noise parameters measured between 2 GHz and 26 GHz can be extrapolated to 60 GHz, and that consistent S-parameters can be obtained for InP HEMT's in precision packages and test fixtures.**

I. Introduction

INDIUM Phosphide-based High Electron Mobility Transistors (InP HEMT's) have demonstrated superior performance as millimeter-wave low-noise amplifiers [1]–[5]. These excellent results point to InP HEMT's as the transistor of choice for critical low-noise applications at millimeter waves. To design an optimum amplifier and avoid costly manual off-chip matching structures, the amplifier designer must know both the scattering parameters and the noise parameters of the transistor. Furthermore, the parameters must be referenced to the terminals of the transistor as it will appear in the integrated circuit. This paper presents techniques for obtaining these design parameters to 60 GHz.

Most millimeter-wave noise figure results reported to date have been obtained for discrete transistors that have been empirically tuned to a minimum noise figure [6], [7]. The empirical technique does not yield the optimum source admittance nor the effective noise resistance, which are also required for design of monolithic millimeter-wave integrated circuits. Low-noise amplifier designs have been based on noise parameters extrapolated from lower frequencies [5] or amplifiers with the input tuned off-chip [8]. At microwave frequencies, methods are well established for measuring noise parameters [9]–[12]. These methods use a tuner to present a range of source admittances to the transistor under test. The noise parameters are then obtained by a fitting procedure. This paper is the first to report on the extension of these procedures for direct measurement of noise parameters to 60 GHz. By developing and applying techniques at V-band we are able to confirm the validity of the widely used microwave extrapolation method.

Manuscript received May 29, 1992; revised November 10, 1994.

The authors are with the Electromagnetics and Reliability Directorate, Rome Laboratory, Hanscom AFB, MA 01730 USA.

IEEE Log Number 9410706.

The procedure we use for directly obtaining the design parameters is outlined in Fig. 1, which also serves as a summary of this paper. The S-parameters of the InP HEMT are obtained by fitting an equivalent circuit model to a number of sets of measured S-parameters. The details of the InP HEMT layout, fabrication, and packaging, all of which must be known for accurate design parameters, are described in Section II. The S-parameter measurement and modeling are described in Section III. To provide accurate data for the noise parameter fitting procedure, we separate the noise figure of the InP HEMT from the noise contributed by the components of the measurement system in which it is embedded according to the equation near the upper left corner of Fig. 1. The noise contributed by the passive embedding elements on the input side of the transistor can be computed from their available gains which, in turn, come from S-parameters. The S-parameters of coaxial components are measured directly on a vector network analyzer. The transition from coaxial connector to microstrip makes each half of the test fixture inherently noninsertable. To characterize these noninsertable components, we make a series of one-port S-parameter measurements with both coaxial and microstrip calibrations, then perform computations to find the two-port S-parameters of the noninsertables. This procedure is described in Section III. To find the noise contributed on the output side of the transistor, we first determine the noise parameters of the receiver which includes both active and passive elements. Then, the noise figure of the InP HEMT itself can be obtained from the overall measured noise figure by solving the equation near the upper left corner of Fig. 1. These computations, which are performed as a function of source admittance, are described in Section IV. Section V describes how noise parameters are fit to subsets of the noise figure data to reduce the influence of experimental uncertainty, thus yielding the final noise parameters.

II. InP HEMT Layout, Fabrication, and Packaging

The low-noise InP HEMT's have 0.15-μm gate length with source-to-gate spacing of 0.5 μm and source-to-drain spacing of 2.0 μm. The topology has two parallel gate stripes. InP HEMT's with two different gate widths, 48 and 64 μm, were measured. Connections to the gate and drain electrodes are made through 50-Ω microstrip lines and linear tapers. These lines and tapers establish a microstrip environment for the InP HEMT, the same environment that the transistor will encounter in a monolithic integrated circuit amplifier. The lines and tapers can be de-embedded from the S-parameter and noise parameter measurements as explained below to yield param-

0018–9480/95$04.00 © 1995 IEEE

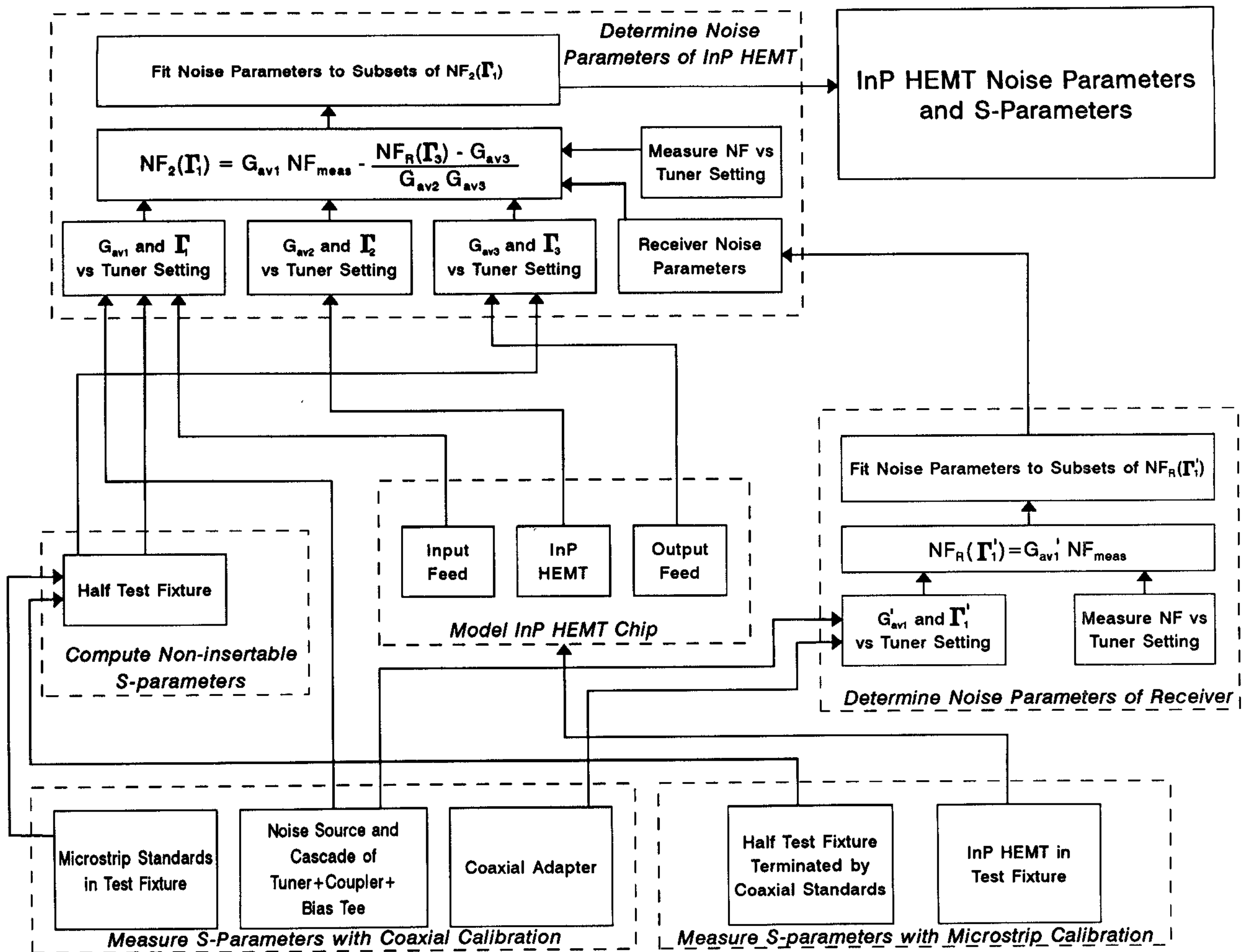

Fig. 1. Flow chart showing major steps for directly determining noise and S-parameters to 60 GHz.

eter values referred to the transistor terminals. Sources are grounded by vias through the 100-μm-thick indium phosphide substrates.

The InP HEMT heterostructure was optimized for low-noise operation at 60 GHz [4], [6]. The lattice-matched structure consists of a superlattice buffer, InGaAs channel, AlInAs spacer, donor and Schottky layers, and an InGaAs contact layer. Typical dc transconductance is 730 mS/mm with F_t of 118 GHz.

We used two types of test fixture for measuring the InP HEMT's: precision millimeter-wave test packages and commercially available millimeter-wave test fixtures [13]. Each type is designed to allow network analyzer calibration to the edge of the semiconductor chip [14]; however, they use different calibration methods as described in Section III. We use data collected from both types in our design database in order to compare the two approaches and to reduce the effects of experimental uncertainty.

The InP HEMT chips were individually mounted, either in a test package or on a chip carrier. The precision package consists of a gold-plated machined brass housing, 50-Ω microstrip feeds on 0.254-mm-thick by 3.81-mm-long alumina substrates soldered to the housing, and 1.85-mm connectors with glass beads. Each chip carrier consists of two 50-Ω microstrip feeds on 0.254-mm-thick by 5.0-mm-long alumina substrates soldered to a gold plated Kovar® plate. In both cases, the InP HEMT is epoxy-attached to a pedestal between the alumina feeds. The pedestal brings the surface of the chip into the plane of the alumina microstrip surface. The connection between the alumina microstrip and the indium phosphide microstrip is made by 76-μm ribbon with thermal compression bonds. The width of the bond ribbon is the same as the 76.0-μm 50-Ω feed line on the InP substrate, reducing the effect of the bond discontinuity.

III. S-PARAMETER MEASUREMENT AND MODELING

We perform full S-parameter characterization of the InP HEMT's from 0.2 to 60 GHz on a coaxial vector network analyzer. For the precision package, the analyzer is calibrated to the end of the alumina feed lines using a set of precision microstrip standards consisting of a thru, a short, and offset shorts. Because each offset short is an effective standard over only a limited bandwidth, we use several offsets to cover this frequency range [15]. As with the InP HEMT's, microstrip standards are individually packaged in precision-machined housings with coaxial-to-microstrip transitions. Wrap-around grounds are used for shorted microstrips. The technique for accurate characterization of these standards has been reported

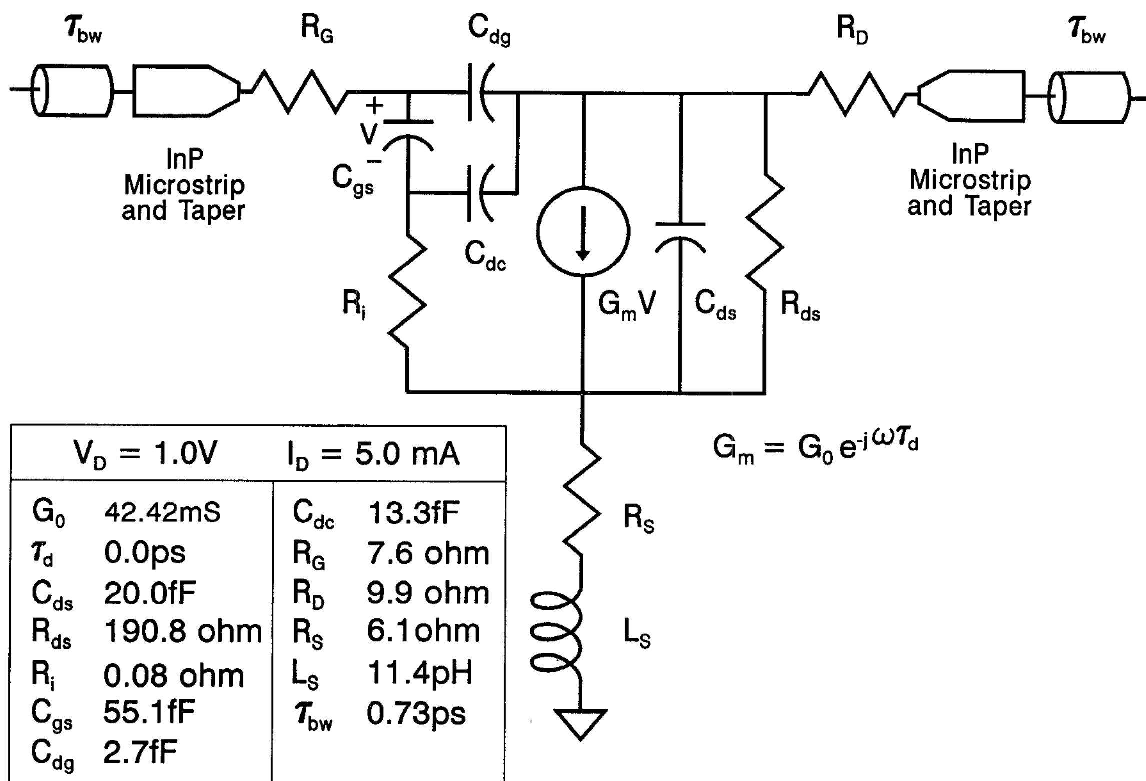

Fig. 2. Circuit model of InP HEMT with bond wires and microstrip feeds.

TABLE I
InP HEMT Bias Points

Total Gate Width	48 μm	64 μm
V_D (V)	I_D (mA)	
1.2	5.0	8.0
1.0	13.0	22.0
1.0	8.0	12.0
1.0	5.0	8.0
0.8	5.0	8.0

[14]. For the commercial fixture, the analyzer is calibrated using the Line–Reflect–Match (LRM) and Line–Reflect–Line (LRL) techniques [16], [17], with microstrip standards provided by the manufacturer. In this case, the coaxial connectors and transitions of the fixture are common to all of the standards. The length of the chip carrier alumina results in the measurement plane being at the edge of the chip.

The InP HEMT S-parameters are used to determine a design model which represents the transistor as it would perform in a monolithic circuit made by the same fabrication process. Since the design model must be representative of the process, it is fit simultaneously to several sets of S-parameter data collected from a number of transistors, at a number of bias points, and over a broad frequency range, using both the precision packages and the commercial fixture. The model topology, shown in Fig. 2, contains thirteen unknown elements: twelve associated with the transistor itself and one associated with the packaging. In addition, the microstrip transmission lines and tapers are represented by standard models, using the physical dimensions of the gold-plated photolithographic structures with a substrate thickness of 100 μm and a dielectric constant 12.4. The variable associated with the packaging is the delay of the 50-Ω transmission lines which represent the bond ribbons and correct for tolerance variations in chip carrier length.

Through a combination of extraction and optimization, a separate model is fit to the S-parameter data for each of the bias points shown in Table I. The optimizer chooses values for the bias dependent elements $G_0, C_{gs}, R_{ds}, C_{dg}$, and R_i at each bias point. The elements C_{dc}, C_{ds}, τ_d, and τ_{bw} are not dependent on bias over the given range and the optimizer finds values for C_{dc}, C_{ds}, and τ_d that are common to all models. The optimization process cannot determine unique values for parasitic elements R_G, R_D, R_S, and L_S so a microwave frequency extraction technique [18], [19] was used to help fix their values. Element values for the model of the 0.15 × 48 μm InP HEMT are listed in Fig. 2. Measured S-parameters

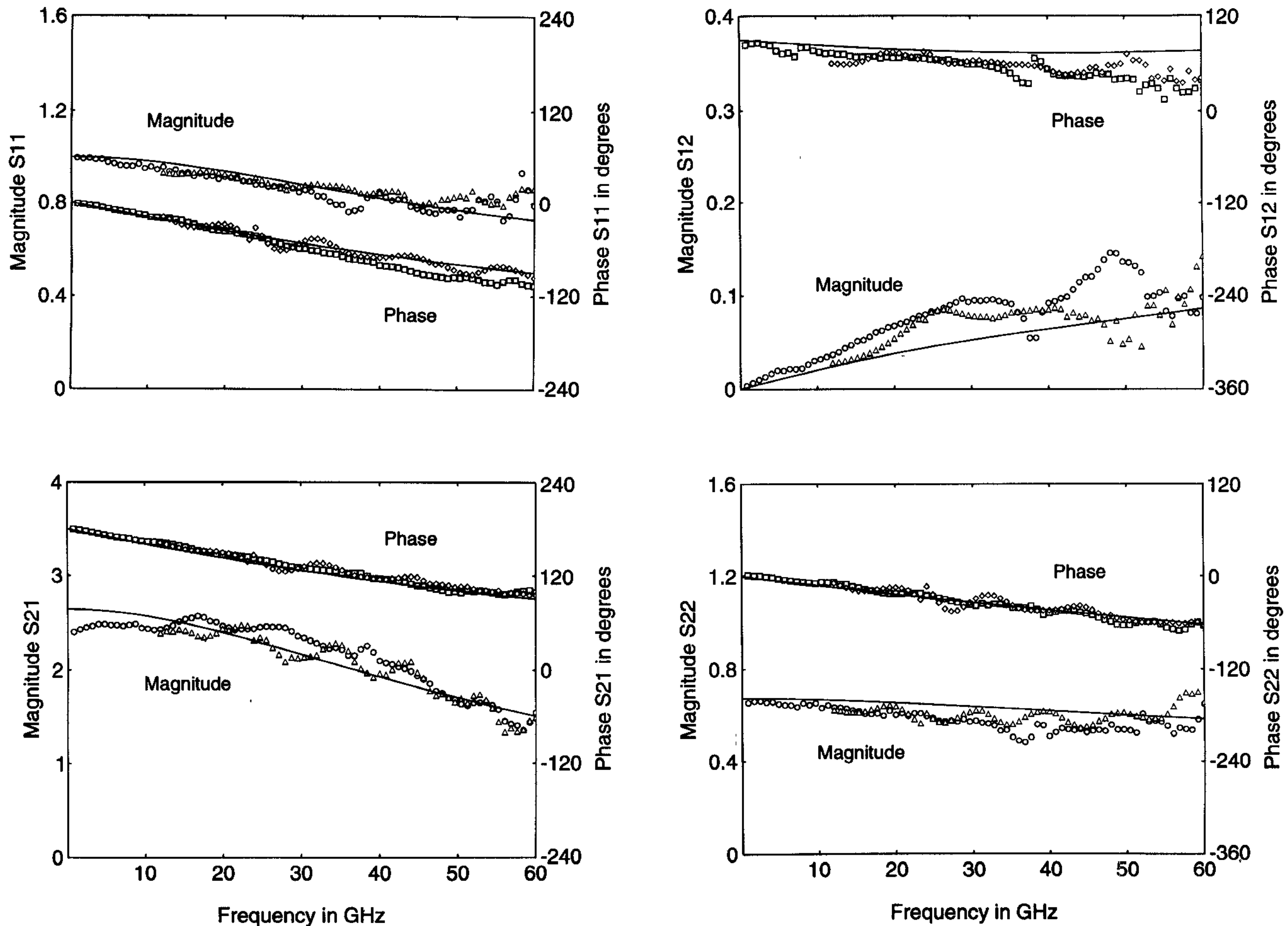

Fig. 3. S-parameters of InP HEMT with $V_D = 1.0$ V and $I_D = 5.0$ mA. Solid lines represent the model. Measurements made in the precision package are shown with triangles for magnitude and diamonds for phase. Measurements made on chip carriers are shown with circles for magnitude and squares for phase.

for both the precision package and the commercial fixture compare equally well with the model as shown in Fig. 3. This is significant because it indicates that accurate measurements can be made where separately packaged calibration standards and Devices Under Test (DUT's) are necessary.

IV. Measuring Noise Figure and Source Admittance

The noise figure of a two-port as a function of source admittance is given by the well-known formula [20]

$$\mathrm{NF}\,(Y_S) = \mathrm{NF}_{\min} + \frac{R_n}{G_S}|Y_S - Y_{\mathrm{opt}}| \qquad (1)$$

where $\mathrm{NF}\,(Y_S)$ is the noise figure of the two-port at source admittance $Y_S = G_S + jB_S$. $\mathrm{NF}_{\min}$ is the minimum noise figure obtained at the optimum source admittance $Y_{\mathrm{opt}} = G_{\mathrm{opt}} + jB_{\mathrm{opt}}$, and R_n is the effective noise resistance, a measure of how rapidly the noise figure grows as the source admittance moves away from Y_{opt}. We obtain the four noise parameters, $\mathrm{NF}_{\min}, G_{\mathrm{opt}}, B_{\mathrm{opt}}$, and R_n at each frequency of interest by fitting the noise figure of the transistor at a number of distinct source admittances. We fit noise parameters to noise figures based on the methods described by Lane [21] and by Mitama and Katoh [22]. The fit requires accurate measurement of both noise figure and source admittance.

Fig. 4 is a block diagram of the noise figure measurement system. The coaxial noise source feeds the coupled port (port 3) of a −3-dB directional coupler through a coaxial-to-waveguide transition. The coupler directs the noise to the transistor chip through a waveguide-to-coaxial transition attached to port 2. A terminated E-H tuner at port 1 of the coupler provides the variable source admittance. With this arrangement, the coupler presents to the noise source a relatively constant load, S_{33}, and transmission parameter, S_{32}, while the transistor under test sees a variable source admittance, S_{22}. A coaxial bias tee is used between the coupler and the InP HEMT test fixture for application of gate bias.

Following the transistor test fixture are a coaxial bias tee for drain bias, a monolithic three-stage InP HEMT low-noise amplifier in a coaxial package, a coaxial-to-waveguide transition, a single-sideband downconverter, and a microwave noise figure measurement system. The V-band low-noise amplifier is similar to an earlier two-stage design [1] and improves the noise figure measurement accuracy by suppressing the noise contribution of the components that follow the amplifier. The downconverter consists of a mixer with synthesized local oscillator in the 35–45-GHz range to downconvert the V-band test noise. The lower sideband of this conversion at 20–30 GHz is filtered out by the V-band waveguide below cutoff. At the 15.5-GHz first IF frequency, the test noise is amplified

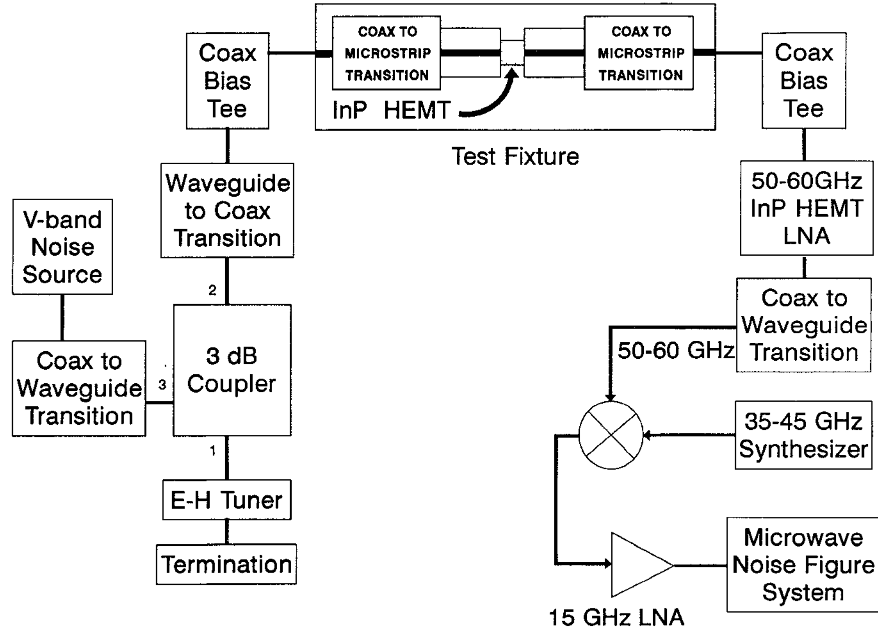

Fig. 4. Block diagram of noise figure measurement system.

by 30 dB in an amplifier with 1.8-dB noise figure. The 15.5-GHz test noise is then applied to a microwave noise figure measurement system.

To obtain the noise of the InP HEMT alone, the contribution of the embedding components must be removed from the measured data. The fundamental equation for de-embedding the noise figure of the transistor under test from the measured noise figure is the cascade noise equation [23]

$$\begin{aligned}\mathrm{NF}_{\mathrm{meas}} =& \mathrm{NF}_1 + \frac{\mathrm{NF}_2 - 1}{G_{av1}} + \frac{\mathrm{NF}_3 - 1}{G_{av1}G_{av2}} \\ &+ \frac{\mathrm{NF}_4 - 1}{G_{av1}G_{av2}G_{av3}}. \end{aligned} \tag{2}$$

Here $\mathrm{NF}_{\mathrm{meas}}$ is the noise figure of the entire measurement cascade, NF_1 is the noise figure of the input embedding network, NF_2 is the noise figure of the InP HEMT, NF_3 is the noise figure of the output embedding network, NF_4 is the noise figure of the noise receiver, and the $G_{avi}, i = 1, 2, 3,$ are the corresponding available gains.

On the input side, the de-embedding must remove the contribution of the networks between the noise source Excess Noise Ratio (ENR) calibration plane and the transistor gate terminal. These are passive networks whose noise figure can be expressed as the inverse of their available gain [24]. Obtaining accurate two-port S-parameters to compute the available gain of the input and output networks is complicated by the coaxial-to-microstrip transitions. Since these components are inherently noninsertable, measuring them on a network analyzer with full two-port calibration is impossible [25]. To overcome this difficulty, we employ the following technique.

A one-port calibration of the network analyzer is performed using calibration standards appropriate for port 1 of the unknown network. The two-port is converted to a one-port by attaching each of three different standards to port 2. Network analyzer measurements yield three reflection coefficients, Γ_{mi}, which can be expressed in terms of the unknown two-port S-parameters and the known reflection coefficients of the three different standards, Γ_i as follows:

$$\Gamma_{mi} = S_{11} + \frac{S_{21}S_{12}\Gamma_i}{1 - S_{22}\Gamma_i}, \qquad i = 1, 2, 3. \tag{3}$$

This system of equations is solved to obtain (4)–(6), shown at the bottom of this page, where

$$\begin{aligned}\Delta =& \Gamma_2\Gamma_3(\Gamma_{m2} - \Gamma_{m3}) + \Gamma_3\Gamma_1(\Gamma_{m3} - \Gamma_{m1}) \\ &+ \Gamma_1\Gamma_2(\Gamma_{m1} - \Gamma_{m2}). \end{aligned} \tag{7}$$

$$S_{11} = \frac{\Gamma_2\Gamma_3\Gamma_{m1}(\Gamma_{m2} - \Gamma_{m3}) + \Gamma_3\Gamma_1\Gamma_{m2}(\Gamma_{m3} - \Gamma_{m1}) + \Gamma_1\Gamma_2\Gamma_{m3}(\Gamma_{m1} - \Gamma_{m2})}{\Delta} \tag{4}$$

$$S_{22} = -\frac{\Gamma_1(\Gamma_{m2} - \Gamma_{m3}) + \Gamma_2(\Gamma_{m3} - \Gamma_{m1}) + \Gamma_3(\Gamma_{m1} - \Gamma_{m2})}{\Delta} \tag{5}$$

and

$$S_{21}S_{12} = \frac{\Gamma_1\Gamma_{m1}(\Gamma_{m2} - \Gamma_{m3}) + \Gamma_2\Gamma_{m2}(\Gamma_{m3} - \Gamma_{m1}) + \Gamma_3\Gamma_{m3}(\Gamma_{m1} - \Gamma_{m2})}{\Delta} + S_{11}S_{22} \tag{6}$$

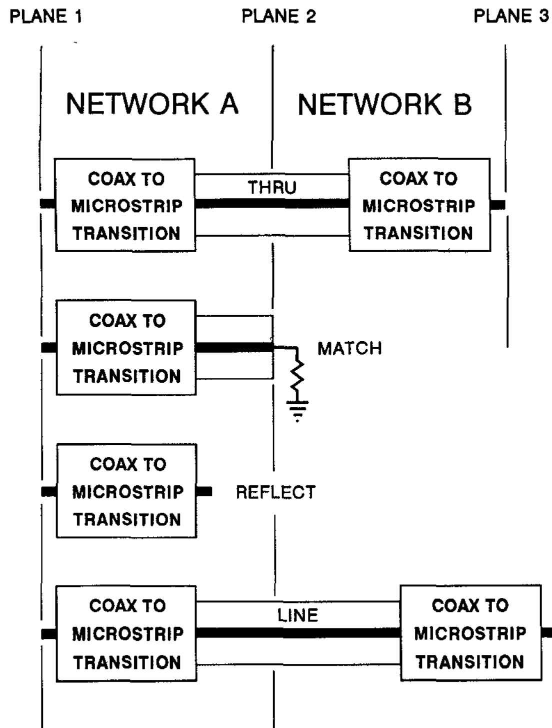

Fig. 5. Noninsertable two-port networks are characterized by converting them to one-port networks.

Finally, since our unknown two-port is reciprocal

$$S_{12} = S_{21} = \sqrt{S_{21}S_{12}}. \qquad (8)$$

Consider, for example, the network shown at the top of Fig. 5, which represents the test fixture consisting of a coaxial-to-microstrip transition, a microstrip delay line, and a microstrip-to-coaxial transition. We can characterize the output half of this network, which we call network B, as follows. First, calibrate the network analyzer using the LRM microstrip calibration standards described in Section III. This calibration establishes plane 2 as the reference plane. (Note that this is the plane at which the InP HEMT is connected in Fig. 4.) The microstrip through line is then mounted in the fixture, but the calibration ensures that the measurement reference plane corresponds to the end of the alumina microstrip feed line of the transistor chip carrier. Using a coaxial short, open, and matched load at plane 3 as the second set of standards, we measure the unknown network three times and solve (3) for the two-port S-parameters.

Similarly, for network A in Fig. 5, we calibrate the network analyzer with coaxial standards, then measure with LRM microstrip standards connected at plane 2. Fig. 6 shows the excellent agreement obtained when we cascade the individually computed S-parameters of networks A and B, and compare the result to the direct two-port coaxial S-parameter measurement of the microstrip through in the test fixture.

The coaxial-to-waveguide transition, the coupler–tuner–termination combination, the waveguide-to-coaxial transition, and the bias tee, form a coaxial two-port that can be accurately measured by an automatic network analyzer. We measured the two-port S-parameters of this component over the range of tuner settings to determine the region of the source admittance plane available for noise parameter fitting. Noise figure measurements were typically performed at 25 source admittances.

To obtain the noise figure of the InP HEMT at the gate terminal, the input network must also include the bond ribbon, the on-chip microstrip feed line, and the linear taper. These are included in a straightforward manner by cascading S-parameters computed from the models in Fig. 2.

On the output side of the HEMT, the third stage is a cascade of the linear taper, on-chip microstrip feed line, bond ribbon, and the output half of the package, network B above. Again, the available gain and noise figure can be computed from S-parameters.

The fourth stage is the noise receiver defined with its input port at the input of the drain bias tee. It includes both active and passive networks. To find the noise figure, $\mathrm{NF}_R = \mathrm{NF}_4$, we first determine the noise parameters of the receiver. We can then compute the noise figure of the receiver as a function of the output reflection coefficient of the third stage during InP HEMT measurement. We determine receiver noise parameters by using a coaxial adapter in place of the test fixture and measuring the noise figure of the entire measurement system as a function of tuner setting. Here, the receiver can be considered the second of two stages in the measurement system, where the first stage is the cascade of the coupler–tuner–bias tee and coaxial adapter. For two stages, (2) reduces to

$$\mathrm{NF}_R(\Gamma_1') = G_{av1}' \, \mathrm{NF}_{\mathrm{meas}}. \qquad (9)$$

Here, Γ_1' is the source reflection coefficient seen by the receiver and G_{av1}' is the available gain of the first stage including the coaxial adapter. Γ_1' and G_{av1}' are computed from measured S-parameters. Knowing noise figure as a function of source reflection coefficient, we can find the noise parameters of the receiver by the fitting procedure that will be described in Section V.

Equation (2) can now be solved for the noise figure of the transistor under test in terms of the measured noise figure, the available gains, and the noise figure of the receiver

$$\mathrm{NF}_2(\Gamma_1) = G_{av1}\mathrm{NF}_{\mathrm{meas}} - \frac{\mathrm{NF}_R(\Gamma_3) - G_{av3}}{G_{av2}G_{av3}}. \qquad (10)$$

G_{av2} is computed from the measured InP HEMT S-parameters with the modeled bond ribbons, feed lines, and tapers removed. The source reflection coefficient Γ_1 seen by the InP HEMT for each tuner setting is computed from the S-parameters of the input network terminated with the measured one-port S-parameters of the noise source. A typical set of 25 source admittances as seen from the gate terminal plane is shown in Fig. 7. Measurements of the real and imaginary parts of the S-parameters of the micrometer-controlled tuner are repeatable to within 0.005. A direct one-port S-parameter measurement of the input network using microstrip calibration (corresponding to measurement plane 2 in Fig. 5) can also be used to determine Γ_1. The S-parameters of the bond wire, on-chip microstrip, and linear taper would be cascaded. These two techniques work equally well for determining Γ_1. The source reflection coefficient seen by the receiver Γ_3 is computed

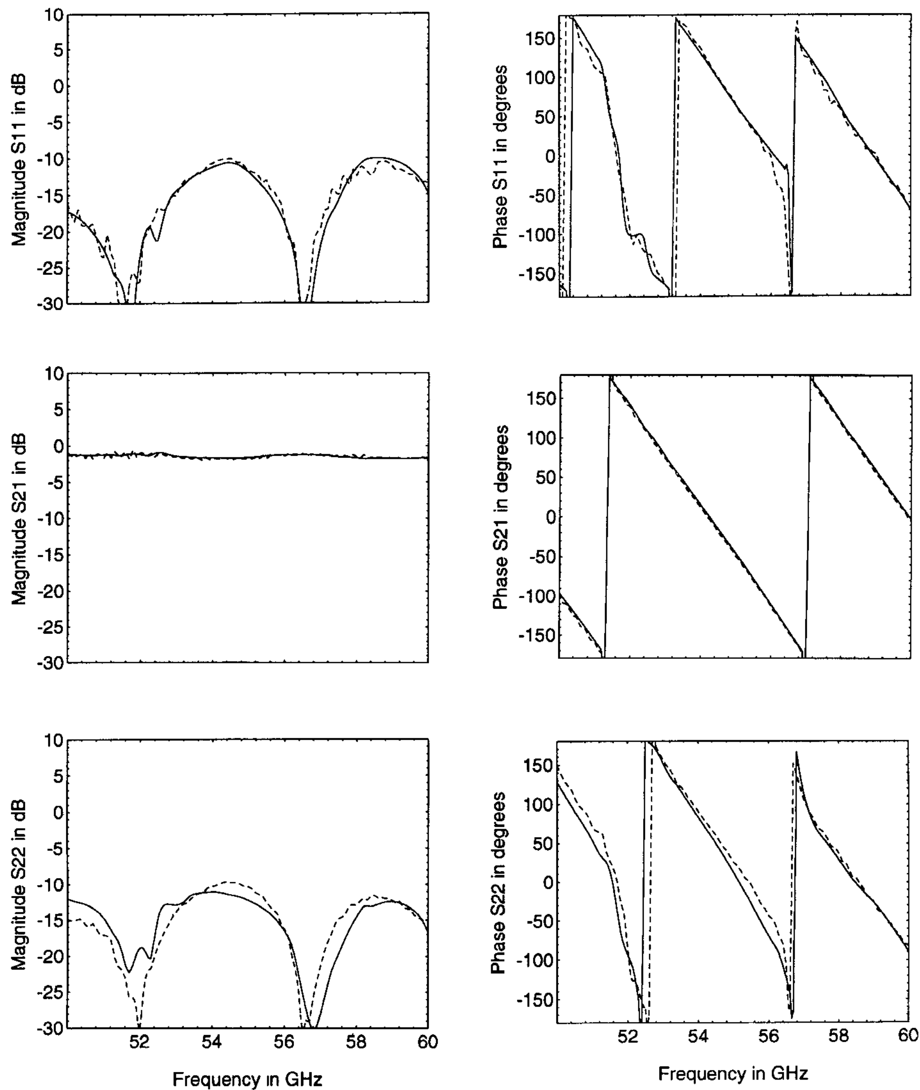

Fig. 6. Comparison of the cascaded computed S-parameters of two noninsertable two-port networks (solid lines) with the directly measured S-parameters of the equivalent insertable two-port (dashed lines).

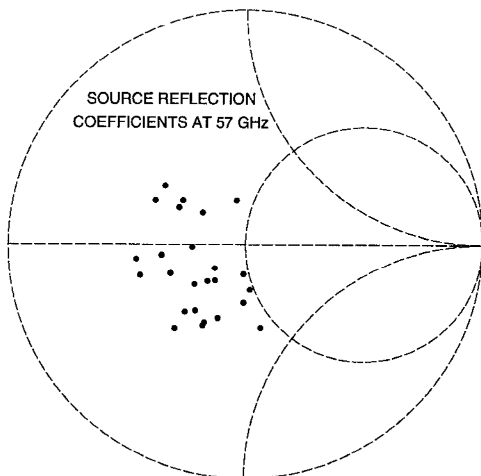

Fig. 7. Distribution of 25 source reflection coefficients presented to the InP HEMT at 57.0 GHz.

from the cascaded S-parameters of the first, second, and third stages terminated by the noise source.

V. Noise Parameters

Fitting noise parameters to the measured noise figures is sensitive to the accuracy of both the measured noise figures and the source admittances. Recall that the noise parameters describe a noise figure paraboloid in the source admittance plane, with its minimum at the optimum source admittance [20]. Ideally, one would measure noise figures over a distribution of source admittances that covered the entire source admittance plane, with several points in the vicinity of the minimum. Loss in the input network compresses the source admittance distribution into a smaller section of the plane which may not be near the minimum. This loss, which generally increases with frequency, makes millimeter-wave noise parameter measurement challenging. The fitted noise paraboloid must be extrapolated to regions of the plane away from the data. Uncertainty in the data points can cause significant variations in the fitted noise parameters, even when the fit to the data is very good. In our case, the loss of the components between the noise source and the transistor test fixture is approximately 7 dB in the 50–60-GHz band.

TABLE II
InP HEMT NOISE PARAMETERS AT 57 GHz. V_D = 1.0 V, I_D = 5.0 mA

parameter	mean	standard deviation
Minimum Noise Figure (dB)	1.37	0.20
Optimum Source Reflection Coefficient		
$\|\Gamma_{opt}\|$	0.40	0.047
$\angle\Gamma_{opt}$	114.60	3.57
Effective Noise Resistance Normalized to 50 Ω	0.64	0.057

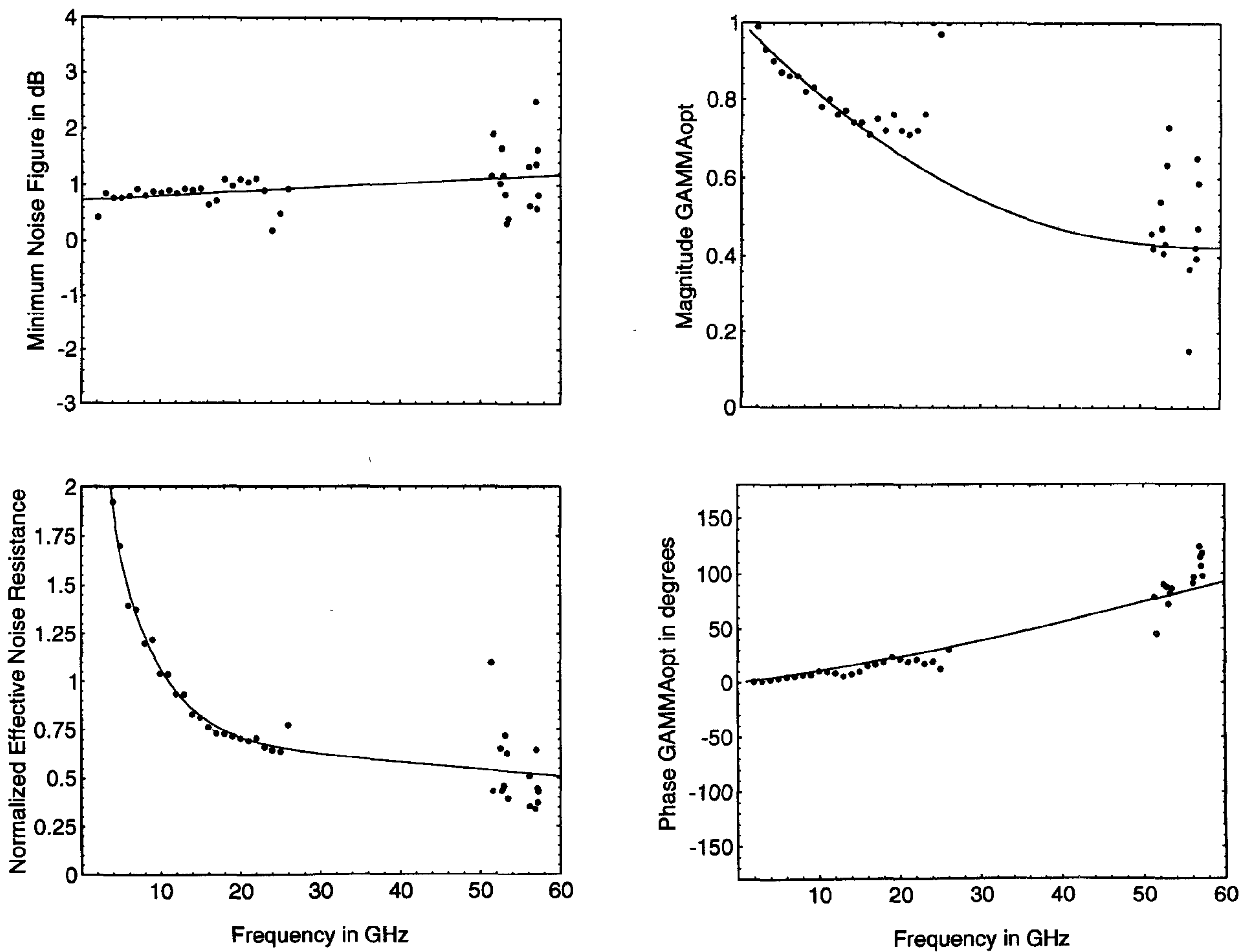

Fig. 8. Measured InP HEMT noise parameter data points and empirical extrapolation from microwave to 60 GHz.

To reduce the distortion in the extrapolation, we systematically exclude source admittances, fit to subsets of the data at each frequency, and compute the mean and standard deviation of the noise parameters. Typically, we fit to all combinations of the 25 source admittances taken 17 at a time, for a total of 480 700 subsets. The fitting can be accomplished in less than 7 min/frequency on a workstation. For some subsets, the fitting algorithm was not successful, terminating prematurely on a nonphysical result, such as an imaginary minimum noise figure. These unsuccessful cases occur for combinations that include inaccurate data. For example, at 57.0 GHz the fit was successful 346 105 times. Only the successful fits are included in the computation of the mean and standard deviation.

In Fig. 8, the noise parameters of a $0.15 \times 48\,\mu$m InP HEMT between 50 and 60 GHz are plotted together with microwave noise parameters (2–26 GHz). The data are referenced to the

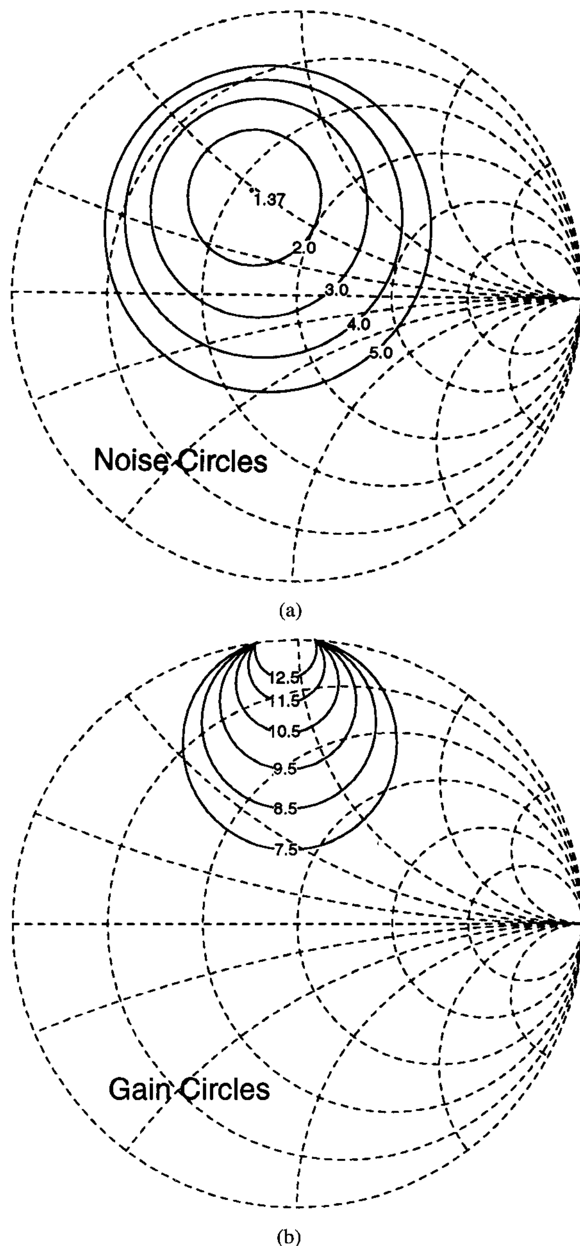

Fig. 9. Noise circles and available gain circles of an InP HEMT at 57.0 GHz. Values are in decibels. $V_D = 1.0$ V, $I_D = 5.0$ mA. Noise parameters correspond to the measurements in Table II and S-parameters to the model in Fig 2.

gate and drain terminals of the InP HEMT and were measured in the commercial fixture. Empirically drawn curves show an extrapolation of the microwave data to 60 GHz. In spite of some scatter in the millimeter-wave experimental data the extrapolation is reasonable.

Noise circles for the InP HEMT at 57.0 GHz are shown in Fig. 9. We chose 57 GHz as being representative of our measured data. The circles correspond to the mean noise parameters listed in Table II along with their standard deviations for the set of 346 105 successful fits. Gain circles computed from the S-parameters of the InP HEMT model are also shown in Fig. 9. The 12.5-dB circle is close to the maximum stable gain of 12.74 dB. The reference planes for these parameters are at the gate and drain terminals of the InP HEMT and represent the transistor as it would appear in a monolithic circuit environment. These parameters are therefore appropriate for the design of monolithic millimeter-wave integrated circuits [1].

VI. Summary and Conclusion

Millimeter-wave techniques for directly obtaining the noise parameters and S-parameters of transistors have been demonstrated. These are the first direct measurements of noise parameters at these frequencies. The detailed description of the techniques should be useful to those needing to make similar measurements. These techniques rely on careful characterization of the measurement system, of the transistor test fixture, and of the transistor itself. Losses in the input network limit the range of source admittances available for fitting noise parameters, but a data selection technique improves the fitting procedure. Our measurements show that noise parameters measured between 2 and 26 GHz can be extrapolated to 60 GHz. In addition, we have shown that S-parameter measurements made on individually packaged InP HEMT's are consistent with measurements made in a commercial test fixture. This is an important result because it is not always practical to use a test fixture.

Since the measurements represent the InP HEMT in the monolithic circuit environment, and the reference planes are at the gate and drain terminals, the resulting parameters are appropriate for the design of monolithic millimeter-wave integrated circuits. The development of the procedure described in this paper led to the successful realization of a 56–60-GHz fully monolithic InP HEMT low-noise amplifier [1]

Acknowledgment

The InP HEMT's used for these measurements were fabricated under contract at Hughes Research Laboratories, Malibu CA, from a layout provided by Rome Laboratory on magnetic tape. The authors wish to thank Dr. L. E. Larson of Hughes for his efforts. Microwave noise parameter measurements were made at ATN Microwave, Inc., Billerica MA, on an NP5B noise parameter measurement system. The authors wish to thank D. Wandrei of ATN for his efforts.

References

[1] R. T. Webster, A. J. Slobodnik, Jr., and G. A. Roberts, "Monolithic InP HEMT V-band low noise amplifier," *IEEE Microwave and Guided Wave Lett.*, vol. 2, no. 6, pp. 236–238, 1992.

[2] R. Lai, H. Wang, K. L. Tan, D. C. Streit, P. H. Liu, J. Velebir, Jr., S. Chen, J. Berenz, and M. W. Pospieszalski, "A monolithically integrated 120-GHz InGaAs/InAlAs/InP HEMT amplifier," *IEEE Microwave Guided Wave Lett.*, vol. 4, no. 6, pp. 194–195, 1994.

[3] R. Lai, K. W. Chang, H. Wang, K. Tan, D. C. Lo, D. C. Streit, P. H. Liu, R. Diz, and J. Berenz, "A high performance and low DC power V-band MMIC LNA using 0.1 μm InGaAs/InAlAs/InP HEMT technology," *IEEE Microwave and Guided Wave Lett.*, vol. 3, no. 12, pp. 447–449, 1993.

[4] S. E. Rosenbaum, K. Litvin, C. S. Chou, L. E. Larson, L. D. Nguyen, C. Ngo, M. Lui, J. Henige, M. A. Thompson, U. Mishra, and D. Pierson, "AlInAs/GaInAs on InP HEMT low noise MMIC amplifiers," in *1991 IEEE MTT-S Int. Microwave Symp. Dig.*, Boston, MA, June 1991, pp. 815–817.

[5] K. H. G. Duh, P. C. Chao, S. M. J. Liu, P. Ho, M. Y. Kao, and J. M. Ballingall, "A super low-noise 0.1 T-gate InAlAs-InGaAs-InP HEMT,"

IEEE Microwave and Guided Wave Lett., vol. 1, no. 5, pp. 114–116, 1991.
[6] U. K. Mishra, A. S. Brown, M. J. Delaney, P. T. Greiling, and C. F. Krumm, "The AlInAs-GaInAs HEMT for microwave and millimeter-wave applications," *IEEE Trans. Microwave Theory Tech.*, vol. 37, no. 9, pp. 1279–1285, 1989.
[7] K. L. Tan, R. M. Dia, D. C. Streit, L. K. Shaw, A. C. Han, M. D. Sholley, P. H. Liu, T. Q. Trihn, T. Lin, and H. C. Yen, "60-GHz pseudomorphic $Al_{0.25}Ga_{0.75}As/In_{0.28}Ga_{0.72}As$ low-noise HEMT's," *IEEE Electron Dev. Lett.*, vol. 12, no. 1, 1991.
[8] P. M. Smith, P. C. Chao, P. Ho, K. H. Duh, M. Y. Kao, J. M. Ballingall, S. T. Allen, and A. Tessmer, "Microwave InAlAs/InGaAs/InP HEMTs: Status and applications," in *2nd Int. Conf. on Indium Phosphide and Related Materials*, Denver, CO, 1990, pp. 39–43.
[9] V. Adamian, "Test set gauges noise parameters from 6–18 GHz," *Microwaves & RF*, vol. 27, pp. 259–261, May 1988.
[10] A. C. Davidson, B. W. Leake, and E. Strid, "Accuracy improvements in microwave noise parameter measurements," *IEEE Trans. Microwave Theory Tech.*, vol. 37, no. 12, pp. 1973–1977, 1989.
[11] J. W. Archer and R. A. Batchelor, "Fully automated on-wafer noise characterization of GaAs MESFET's and HEMT's," *IEEE Trans. Microwave Theory Tech.*, vol. 40, no. 2, pp. 209–216, 1992.
[12] R. A. Pucel, W. Struble, R. Hallgren, and U. L. Rohde, "A general noise de-embedding procedure for packaged two-port linear active devices," *IEEE Trans. Microwave Theory Tech.*, vol. 40, no. 11, pp. 2013–2017, 1992.
[13] *3680 Series Universal Test Fixture Operation and Maintenance Manual*, Anritsu-Wiltron, Morgan Hill, CA.
[14] A. J. Slobodnik, Jr., R. T. Webster, G. A. Roberts, and G. J. Scalzi, "Millimeter wave GaAs switch FET modeling," *Microwave J.*, vol. 32, no. 8, pp. 93–104, 1989.
[15] G. J. Scalzi, A. J. Slobodnik, Jr., G. A. Roberts, "Network analyzer calibration using offset shorts," *IEEE Trans. Microwave Theory Tech.*, vol. 36, no. 6, pp. 1097–1100, 1988.
[16] H. J. Eul and B. Shiek, "Thru-match-reflect: One result of a rigorous theory for de-embedding and network analyzer calibration," in *Proc. 18th European Microwave Conf.*, Stokholm, Sweden, 1988, pp. 909–914.
[17] G. F. Engan and G. A. Hoer, "Thru-reflect-line: An improved technique for calibrating the dual 6-port automatic network analyzer," *IEEE Trans. Microwave Theory Tech.*, vol. MTT-27, no. 12, pp. 987–993, Dec. 1979.
[18] G. Dambrine, A. Cappy, F. Heliodore, and E. Playez, "A new method for determining the FET small-signal equivalent circuit," *IEEE Trans. Microwave Theory Tech.*, vol. 36, no. 7, pp. 1151–1159, July 1988.
[19] A. Eskandarian and S. Weinreb, "A note on experimental determination of small-signal equivalent circuit of millimeter-wave FETs," *IEEE Trans. Microwave Theory Tech.*, vol. 41, no. 1, pp. 159–162, Jan. 1993.
[20] H. Fukui, "Available power gain, noise figure, and noise measure of two-ports and their graphical representations," *IEEE Trans. Circuit Theory*, vol. CT-13, pp. 137–142, June 1966.
[21] R. Q. Lane, "The determination of device noise parameters," *Proc. IEEE*, vol. 57, no. 8, pp. 1461–1462, 1969.
[22] M. Mitama and H. Katoh, "An improved computational method for noise parameter measurement," *IEEE Trans. Microwave Theory Tech.*, vol. MTT-27, no. 6, pp. 612–615, June 1979.
[23] H. T. Friis, "Noise figures of radio receivers," *Proc. IRE*, vol. 32, no. 7, pp. 419–422, 1944.
[24] M. W. Pospieszalski, "On the noise parameters of isolator and receiver with isolator at the input," *IEEE Trans. Microwave Theory Tech.*, vol. MTT-34, no. 4, pp. 451–453, 1986.
[25] R. P. Meys, "A triple through method for characterizing test fixtures," *IEEE Trans Microwave Theory Tech.*, vol. 36, no. 6, pp. 1043–1046, 1988.

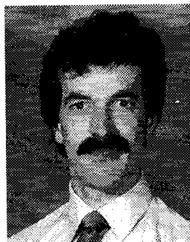

Richard T. Webster (S'76–M'76–M'81) received the B.S. and M.E. degrees in electrical engineering from Rensselaer Polytechnic Institute, Troy, NY, in 1973 and 1976, respectively.

In 1980, he joined what is now the Electromagnetics and Reliability Directorate of Rome Laboratory at Hanscom AFB, MA. His work in the Component Technology Branch has included research on surface acoustic waves (SAW's), the interaction of SAW's with semiconductors, and most recently, the development of monolithic microwave and millimeter-wave integrated circuits. He is the author of a number of technical publications and presentations in these areas.

Mr. Webster is a member of Sigma Xi.

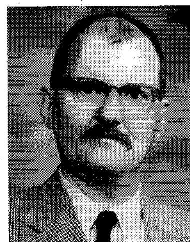

Andrew J. Slobodnik, Jr. (S'65–M'68) received the B.S. and M.S. degrees in electrical engineering from the Massachusetts Institute of Technology, Cambridge, in 1966.

After an additional year of graduate study at the University of California, Berkeley, he began working for what is now the Electromagnetics and Reliability Directorate, Rome Laboratory, Hanscom AFB, MA, where he is still employed. He is currently working in the area of monolithic millimeter-wave integrated circuit (MMIC) research and development.

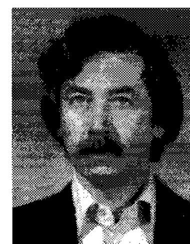

George A. Roberts attended courses in electronics and physics in Northeastern and Boston Universities.

He was employed by Stevens Institute of Technology, Hoboken, NJ, in 1965 to do research in plasma physics at the Air Force Cambridge Research Laboratories (AFCRL). In 1968 he was employed by AFCRL to continue working in the same technical ara. In 1972 he joined what is now the Component Technology Branch of the Rome Laboratory. His current work is in the area of monolithic millimeter-wave integrated circuit research and development.